Physicochem. Probl. Miner. Process., 59(4), 2023, 173554

http://www.journalssystem.com/ppmp

Physicochemical Problems of Mineral Processing

ISSN 1643-1049

Research on deposition of silver nanoparticles at the cellulose/$NaNO_3$ electrolyte interface

Władysław Janusz, Klaudia Kowalska, Ewa Skwarek

Faculty of Chemistry, Maria Curie-Sklodowska University in Lublin; Sq. Maria Curie-Skłodowska 2, Lublin 20-031

Corresponding author: skw3655@umcs.pl (Ewa Skwarek)

Abstract: Currently the research on silver nanoparticles is of great demand owing to their antibacterial properties. One of the possibilities is the study of the silver deposition on the cellulose fibers, and more specifically of the silver nanoparticles and cellulose particles. The research was aimed at obtaining silver nanostructures by reducing ions with formaldehyde and then stabilizing them with the Pluronic solution. A suspension system containing cellulose fibers and silver nanoparticles was prepared in the basic electrolyte $NaNO_3$. There were analyzed the following makes: pH of solutions, grain distribution and zeta potential ζ. Ag nanoparticles are largely applied in medicine, pharmacy, cosmetology and textile industry. Great interest in the nanostructures allows for developing knowledge about them, and thus creating the possibility of further improvement of their properties for subsequent applications.

Keywords: nanomaterials, silver nanoparticles, cellulose, biocomposites

1. Introduction

1.1. Nanoparticles

Nanoparticles and nanomaterials have been the subject of considerable interest among scientists for several decades because of their different properties in relation to materials with larger particle sizes. These materials, with at least one size order smaller than 100 nanometers, are formed from particles obtained under the special pressure or temperature conditions. As a result, atoms are combined in a way different from that in the natural environment. This results in a number of properties that differentiate them from macromolecules, e.g. biocompatibility, hardness, strength, mechanical or chemical resistance (Dębek et al. 2017). Owing to this, it was possible to apply nanomaterials in many fields of industry, starting with the broadly understood chemistry, through the automotive, aviation, armaments industries, and ending with the power industry. In addition to the above-mentioned areas, the use of materials in all branches of medicine is extremely important (Langauer-Lewowicka et al., 2014). The current paper focuses on following changes in the zeta potential of both substrates and the final product of cellulose particles with silver nanoparticles (synthesized from both unfiltered and filtered solutions). Moreover, the cellulose particle sizes and volume distributions for solutions were determined. A diffraction analysis of cellulose samples with nanoAg was conducted out and the degree of crystallinity was calculated. The interaction energy of cellulose particles and Ag nanoparticles was also analysed.

1.2. Nanosilver

Nanosilver, due to its unique properties, is the most commonly used nanomaterial. One of the most important features, which has been used for millennia, has been enhanced owing to the use of nano technology (Rzeszutek et al., 2014). These materials can be obtained in many different ways, however, they can be divided into two main categories: "bottom-up" and "top-down". The first is a chemical method, based on the spontaneous combination of atoms into larger agglomerations. The second mechanism, on the other hand, is based on shredding the material until the desired size is obtained (Runowski, 2014; Pulit et al., 2011).

DOI: 10.37190/ppmp/173554

It has already been proved that nanosilver antipathogenic activity is larger than that of the ordinary silver ions. They can be the best alternative to antibiotics due to the large surface area to the volume ratio and the crystallographic structure of the surface. Some of them are able to develop the antibacterial properties of some antibiotics. The greatest antibacterial properties are used in all sportswear, dressings, detergents and cosmetics. One of the most important applications of nanosilver in medicine are central venous catheters (CVCs). They are frequent sources of infection, which have been partially minimized by the addition of nanoparticles (Burdusel et al., 2018). Besides the antibacterial properties, it is also important to use the antiviral activity of nanosilver, which so far has been used, among others, to suppress the immune deficiency virus (HIV) and hepatitis B virus (HBV). The mechanism of this action is still not fully known. Moreover, the antibacterial properties are largely exploited in the rapid treatment of fungal infections caused by the most common fungi. For this purpose, varnishes, gels and ointments are produced. The research focusing on silver nanoparticles as drug carriers seems promising, as it will improve largely the development of medicine considering significant specificity and selectivity. This is also prospective to focus on the diagnostic and therapeutic aspects of the use of structures in the field of oncology. The researchers' attempts were to enhance radiation and photodynamic therapy as well as to direct drug delivery to cancer cells (Zhang et al., 2016; Biswas et al., 2015).

One example of the use are nanomaterials composed of silver and copper by the metal-metal bonds by means of the technique using silver and copper nanoparticles. The method can be divided into three steps. First, copper oxide nanoparticles are produced by mixing the aqueous solution of $Cu(NO_3)_2$ and NaOH. Then, metallic copper nanoparticles are obtained by reducing copper oxide nanoparticles with hydrazine in the presence of poly(vinylpyrrolidone) (PVP). Finally, the silver/copper nanoparticles are obtained by reducing silver ions with hydrazine in the presence of the metallic copper nanoparticles (Kobayashi et al., 2016). The possibility of deposition of silver nanostructures of various shapes and sizes depending on the surface of the functionalized silica was also investigated. It particular attention was paid to the comprehensive approach to determine pH conditions impact on the metallic nanoparticles (Zienkiewicz-Strzałka, 2018). A relatively novel method is the deposition of silver nanoparticles on the TiO_2 powder using a one-step method involving the cold plasma treatment at the atmospheric pressure. This ensures that the use of environmentally hazardous reducing agents is avoided. The prepared composite has a core-shell structure made of TiO_2 spherical cores and a coating of silver nanoparticles (Skiba 2022).

1.3. Cellulose

Cellulose is an organic compound with the general chemical formula $(C_6H_{10}O_5)_n$, the polysaccharide consisting of repeated glucose units linked by the β-1,4-glycosidic bonds. A single chain can contain from several to hundred thousand glucose units. Cellulose is the building block of cell walls in higher order plants. Cellulose microfibers vary in the diameter, length and complexity depending on the source of their acquisition (Gupta et al., 2017). Obtaining the material can take place mechanically, i.e. obtaining pulp at the atmospheric pressure, or using chemical methods. They can be applied in two ways: the sulphate method (Kraft process) and the sulphite method.

The main advantage of cellulose is its insolubility in water and most organic solvents as well as dilute acids. Due to the fact that it is not digested by humans, it supports peristalsis and intestinal blood supply. In food additives designated E460 as well as in the industry, it is a filler, anti-caking agent and emulsifier (Gupta et al., 2017). It the paper α -cellulose powder, Sigma Life Science (USA) was used. There are many papers dealing with cellulose. Particularly noteworthy is the paper (Lavoine at al., 2012), which presents the definition and description of such a biomaterial in the nanoscale and innovative ways of presenting its new properties.

2. Materials and methods

2.1. Materials

The formaldehyde (Chempur formalin r-r 1%, p.a.), NaOH (Chempur, p.a.) at the concentration of 1.25 mol/dm^3, $AgNO_3$ (Chempur, p.a.), 25% ammonium hydroxide solution (Chempur, p.a.), Pluronic stabilizer (2 g P123/50 cm^3 H_2O) were used for the synthesis of silver nanoparticles (NanoAg). The

decision was made to use this compound due to very effective synthesis, to stabilize is not a waste but directs the structure (Zienkiewicz-Strzałka et al., 2013). $NaNO_3$ electrolyte (Chempur, p.a.) was used to measure the zeta potential ζ of cellulose. pH was examined using a diluted or concentrated HNO_3 solution (Chempur r-r 65%, p.a.) or NaOH. The α -cellulose powder, Sigma Life Science (USA) was used in the paper.

2.2. Methods

Silver nanoparticles (NanoAg) were synthesized reducing the $[Ag(NH_3)^2]^+$ ions with formaldehyde (silver nitrate was the ion source). Synthesis was started from 25 cm^3 of filtered NaOH at the concentration of 1.25 mol/dm^3 was added to 25 cm^3 of filtered $AgNO_3$. The brown Ag_2O precipitate was centrifuged and dissolved in 5.26 cm^3 of 25% ammonium hydroxide solution. Then 130 cm^3 of filtered Pluronic stabilizer was added to the solution followed by the addition of 0.25 cm^3 formaldehyde dropwise. A brown solution of silver nanoparticles was obtained. Before the synthesis there were made, two attempts to obtain NanoAg using unfiltered reagents.

The zeta potential ζ of cellulose (Sigma, degree of polymerization above 200) was measured in the $NaNO_3$ electrolyte for the cellulose samples in $NaNO_3$ at the concentration of 0.001 mol/dm^3, 0.01 mol/dm^3, 0.1 mol/dm^3. To measure the potential of sample no. 1, 100 cm^3 of $NaNO_3$ solution at the concentration of 0.001 mol/dm^3 and 0.01 g of cellulose were placed in the beaker. Then the suspension was sonicated for 3 minutes using the Sonicator XL 2020, Misonix. Then the pH was examined in the range from 2 to 10 using a diluted or concentrated HNO_3 solution or NaOH. The potential values were measured after pH adjustment, from the pH value about 2, then 4, and so on in the rising order to 10. Samples 2 and 3 were treated analogously, changing only the concentration of $NaNO_3$.

The zeta potential ζ of silver nanoparticles was measured at the concentrations like those of cellulose. In order to perform the measurement for sample no. 1, 100 cm^3 of $NaNO_3$ at the concentration of 0.001 mol/dm^3 was placed in a beaker and 100 mm^3 of nanoAg was added dropwise.

In order to test the aggregation of silver nanoparticles on cellulose, 1 g of cellulose weighed into two conical flasks with the volume of 125 cm^3 $NaNO_3$ at the concentration of 0.001 mol/dm^3 was added. 125 mm^3 of silver nanoparticles, obtained by the chemical reduction with formaldehyde, was added dropwise to each flask. The pH=5 value was set for one suspension and pH=9 for the other one.

The cellulose diffraction analysis was performed using the Empyrean, PANalytical X-ray diffractometer. XRD samples were prepared as follows; There were used four flasks to which 1g of cellulose was weighed and the same amount of electrolyte $NaNO_3$ 125 cm^3 was added. Then 0.1% v/v silver nanoparticles were added to two samples and pH was adjusted to 5 and 9, respectively. The fourth sample was prepared in a similar way, only 1% v/v nanoAg was added. Then the samples were placed on a shaker at 22°C for 24 hours, then centrifuged and dried.

Based on the image of cellulose taken under the Quanta3D FEG scanning electron microscope, it can be seen that the particles are characterized by a large then the particle size distribution was measured by the static light scattering using the Malvern Mastersizer 2000.

Using the pH-meter Φ360pH/Temp/mV meter, pH was measured and the grain distribution was examined by the static light scattering using Mastersizer 2000 (Malvern). Next, in order to analyze the zeta potential ζ of cellulose and silver nanoparticles, the measurement was performed using the Zetasizer Nano series (Nano-ZS90) apparatus.

The resulting suspension was subjected to the ultrasounds for 3 minutes using the XL 2020 Sonifier, Misonix. After this time, the pH was set in the range from 2 to 9 using the diluted or concentrated HNO_3 or NaOH solution. The potential values were measured after adjusting the pH value to 2, then 4, and so on in the rising order to 9. The measurement was performed with the Zetasizer Nano series (Nano-ZS90). Samples 2 and 3 were handled analogously changing the concentration of $NaNO_3$. For the samples, the grain size distribution was measured using the static light scattering method with the Malvern Mastersizer 2000 apparatus, and the XRD analysis was performed.

3. Results and discussion

3.1. Cellulose

The specific surface area determined by the nitrogen adsorption-desorption method based on the BET isotherm was 21 m^2/g. Based on the image of cellulose in Fig. 1, it can be seen that the particles are

characterized by a large variety. The selected fibers were measured, the length of the particles was larger than 100 µm, and the width was larger than 16 µm.

The volumetric distribution of cellulose particles for different times of ultrasonic action on the cellulose suspension presented in Fig. 2. indicates that the particle size was between 0.5 µm and 800 µm. As a result of the measurements, the particle fraction from 0.5 to 8 µm, the dominant fraction from 8 to 200 µm and the particle fraction from 200 to 800 µm were obtained.

A diffraction study showed the presence of several peaks characteristic of crystalline cellulose. Fig. 3. presents the diffraction pattern of the cellulose sample.

To determine the degree of crystallinity, the diffraction pattern in Fig. 4. was analyzed using the WaxFit program, the results of the fit are shown in Fig. 5. Then based on the obtained data, the crystallinity coefficients were calculated using the Segal method, taking into account the height of the peak for reflection from the wall 200 and the height of the amorphous peak 2θ=18° (Segal et al., 1959). The degree of crystallinity was 59.6%. It was determined based on the equation:

$$CrI = 100 * (I_{200} - I_{am})/I_{200} \quad (1)$$

where I_{200} –the peak height for the reflection from the wall 200, I_{am} – the amorphous peak height 2θ=18°.

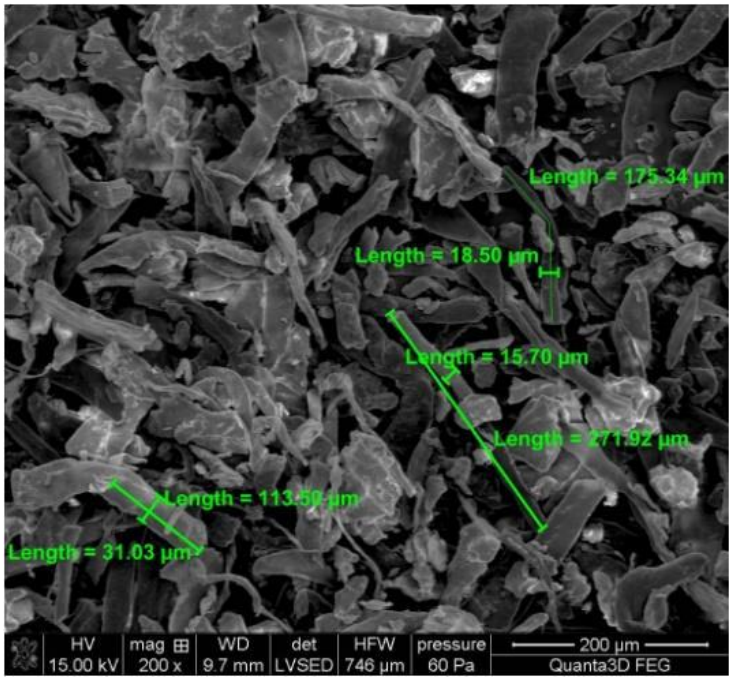

Fig. 1. Sample sizes of cellulose fibers determined by SEM

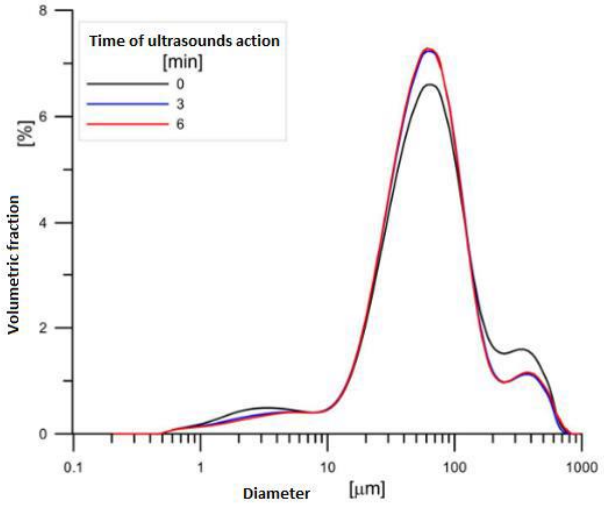

Fig. 2. Volume distribution of cellulose particles

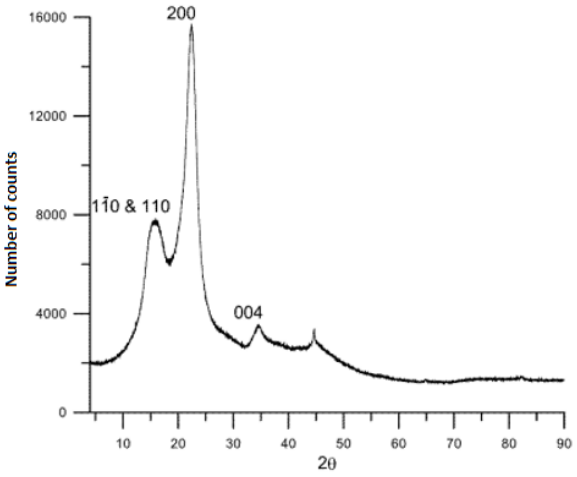

Fig. 3. Powder diffractogram of the cellulose sample

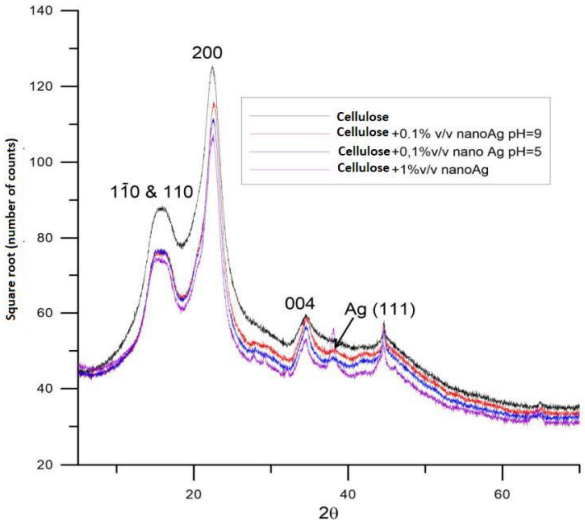

Fig. 4. Powder diffractogram of a cellulose sample with embedded Ag nanoparticles

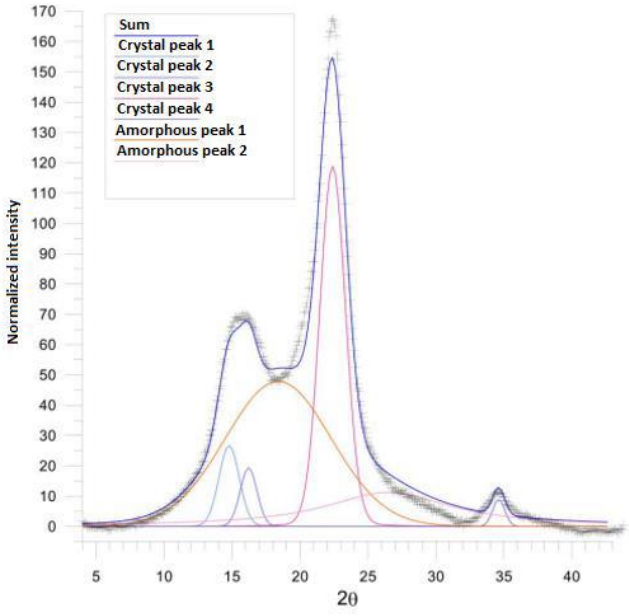

Fig. 5. Matching the diffraction pattern of the cellulose sample to the crystalline and amorphous peaks

To characterize the structure of the cellulose/electrolyte interface, the zeta potential ζ measurements were performed. For the synthesis of nanoAg, for which unfiltered solutions were used, open points were used, for filtered solutions, filled points were used. The measurement results of the zeta potential are presented in the pH range from 2 to 10.5 and the concentrations of the basic electrolyte from 0.01 and 0.1 mol/dm^3 in Fig. 6. An increase in pH causes a decrease in the zeta potential value, which initially in the pH range from 2 to 5.5 is rapid, then at the concentration of 0.001 mol/dm^3 $NaNO_3$ it is mild.

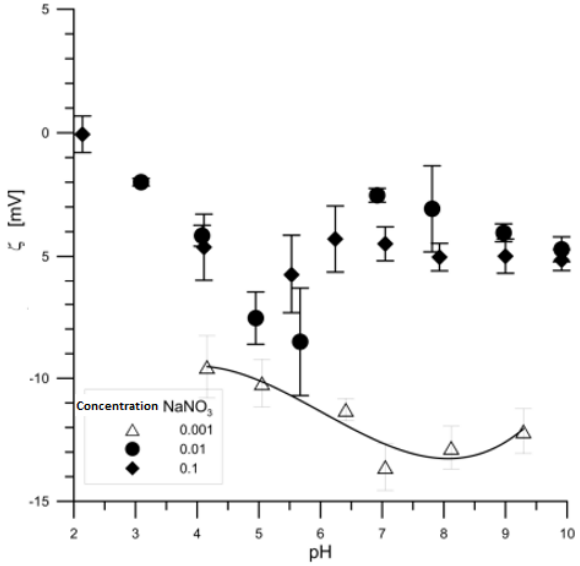

Fig. 6. Cellulose potential as a function of pH and $NaNO_3$ concentration

3.2. Silver nanoparticles

The electrokinetic properties of silver nanoparticles are presented in Fig. 7., showing the dependence of the zeta potential as the function of pH and the concentration of the basic electrolyte. The figure presents the measurement results for both nanoAg syntheses, i.e. for the synthesis in which the solutions were not filtered, for these samples the open points indicate the relationship and the filled ones represent the nanoAg sample obtained from the filtered solutions. For the sample obtained from filtered solutions, the sign of the zeta potential is positive and the values is no changes in the zeta potential with the increasing pH are observed. However, in the case of the synthesis from the unfiltered solutions, there are observed negative zeta potential values decreasing with the pH change.

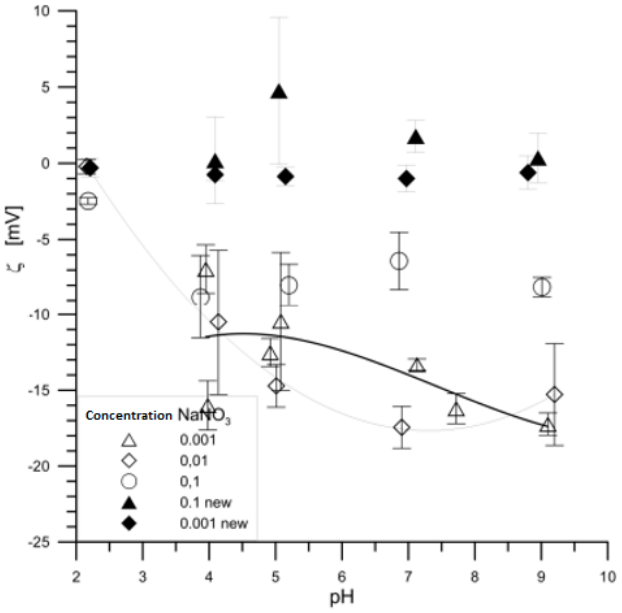

Fig. 7. Zeta potential of Ag nanoparticles as the function of pH and $NaNO_3$ concentration

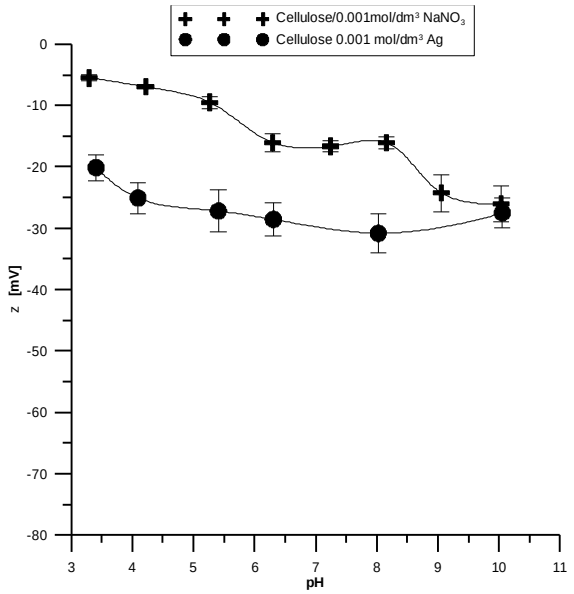

Fig. 8 Dependence of zeta potential on pH for cellulose without and with Ag

Based on Figure 8, it can be concluded that the presence of silver ions in the cellulose suspension affects the value of the zeta potential, the more negative zeta potential is visible in their presence.

3.3. Cellulose particles with embedded silver nanoparticles

After the nanoAg deposition on cellulose, the grain distribution was measured. The results in the form of the dependence of the share of the volume fraction on the diameter of the particles are shown in Fig. 9. The deposition took place at the pH values: 5.5, 7.54 and 9. As follows from the curves of the nanoAg interactions with cellulose, there is no fraction of particles of the sizes of 20 - 280 nm, while the registered grain size distribution is similar to that of cellulose. There is a slight effect of pH on the grain size distribution change and at pH=7.54 the grain size distribution curve is shifted towards the higher diameter values.

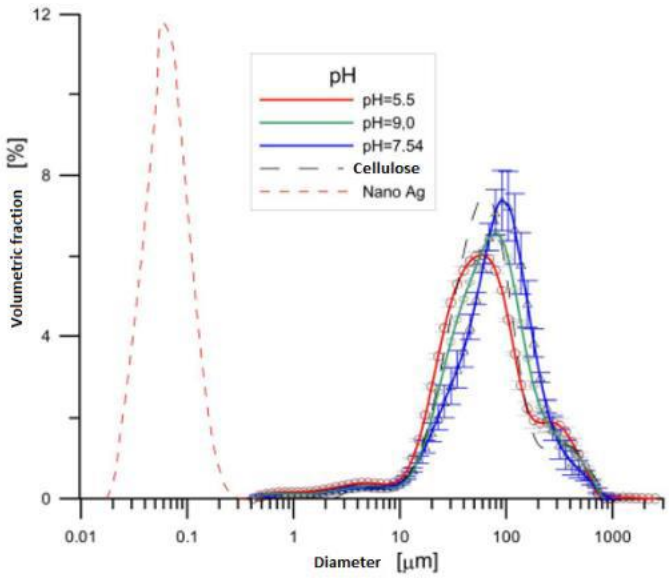

Fig. 9. Decomposition of cellulose particles with the embedded Ag nanoparticles

The analysis of the diffraction pattern for cellulose with the embedded silver nanoparticles at pH=9 with the ratio of the cellulose suspension volume to the nanoAg volume 1000:1, assuming that in the analyzed range of 2θ angles from 4 - 43° shows that there are four crystalline peaks characteristic of

crystalline cellulose, one peak from silver and two amorphous peaks from cellulose. On the basis of the height of the crystalline peak of 200 intensity of cellulose at the angle of 2θ=22.6° and the amorphous cellulose peak of 18.6°, the degree of crystallinity was to be 61% using the Segal method. The comparison of the degree of crystallinity of the initial cellulose sample with that of cellulose with the embedded nanoAg indicates a negligible increase in the degree of crystallinity of the cellulose sample with embedded silver nanoparticles.

In order to determine the stability conditions of the tested system, dispersion and electrostatic interactions were taken into account. Due to the significant difference in the size of cellulose and silver nanoparticles, the ratio of the diameter of the cellulose particle to that of the Ag nanoparticle = 18500/60>100, the system: the spherical nanoAg particle and the flat cellulose particle was used for energy calculations (Gu et al. 1999). The obtained Hamaker's constant for the suspension system containing cellulose particles and silver nanoparticles:

$$A_{102} = (\sqrt{A_{11}} - \sqrt{A_{00}})(\sqrt{A_{22}} - \sqrt{A_{00}}) \quad (2)$$

where A_{11} – the Hamaker's constant for cellulose, A_{22} - the Hamaker's constant for silver, A_{00} - the Hamaker's constant for water was $1.36 \cdot 10^{-20}$. Based on these values and the zeta potential ones at pH=5 and pH=9, the values of the interaction energies of cellulose particles and Ag nanoparticles were calculated. The calculated relationships are shown in Figs. 10. and 11. for pH=5.5 and pH=9.

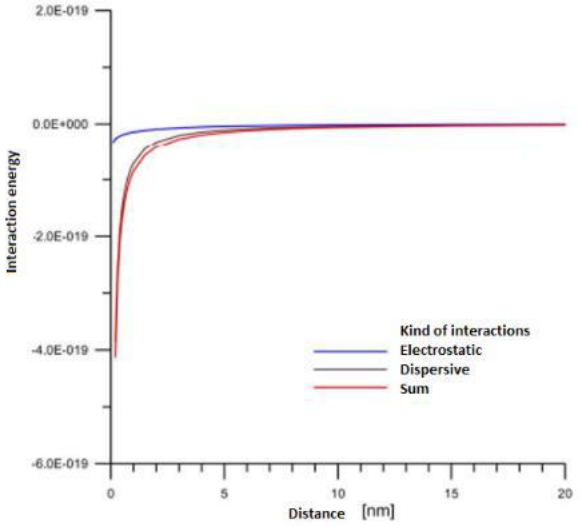

Fig. 10. Energy of electrostatic and dispersion interactions and the total energy according to the DLVO theory of cellulose and nano Ag particles in the suspension at pH=5

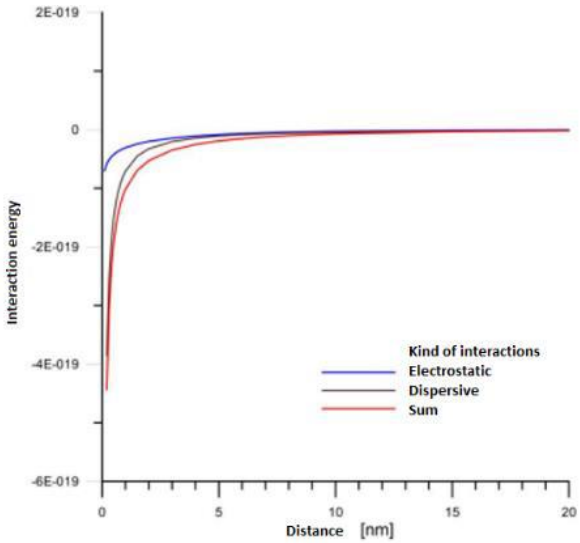

Fig. 11. Energy of electrostatic and dispersion interactions and the total energy according to the DLVO theory of cellulose and nano Ag particles in the suspension at pH=9

The total energy of interactions is close to that of dispersion interactions, while the electrostatic interactions are too weak and do not inhibit aggregation. The results confirm grain distributions and powder diffraction patterns.

4. Conclusions

These results indicate the accumulation of a negative charge on the cellulose surface as a result of the dissociation of acidic groups. The decrease in the absolute values of the zeta potential indicates the complexation reactions taking place on the surface with the participation of the carrier electrolyte ions. The zeta potential of the cellulose suspension with nanoAg obtained using the filtered solutions has a positive sign and a small value. No changes in the pH function are observed. In the case of the synthesis from the unfiltered solutions there are observed, negative zeta potential values, which decrease with the pH change, indicating that the process of obtaining silver nanoparticles has a decisive effect on their surface properties and impurities can affect evidently the zeta potential value. The volumetric grain size distribution of the cellulose suspension was measured for different times of ultrasonic exposure. The size of cellulose particles ranges from 0.5 to 800 μm, of which there can be distinguished three main fractions: from 0.5 to 8 μm, from 8 to 200 μm (dominant) and from 200 to 800 μm. The action of ultrasounds causes a visible dispersion of aggregates with the sizes from 200 to 800 μm and the share in the distribution decreases, while the share of fractions from 10 to 200 μm increases. The grain analysis of nanoAg obtained using the unfiltered solutions showed the presence of three fractions, of which the largest percentage share was in the fraction from 25 to 300 μm. The size distribution of nanoAg particles obtained using the filtered reagents is monomodal and ranges from 20 to 280 nm. 10% of the particle population is below 37 nm, 50% below 69 nm and 90% below 120 nm. The grain distribution of cellulose particles with the embedded Ag nanoparticles is similar to the grain distribution of cellulose. The diffraction analysis of cellulose samples with nanoAg at the ratio of cellulose suspension volume to the nanoAg volume of 1000:1 showed that in the analyzed range of 2θ angles from 4 - 43° there are four peaks characteristic of crystalline cellulose, one silver peak and two amorphous cellulose peaks. On the basis of the obtained heights of the crystalline peaks, the degree of cellulose crystallinity was calculated using the Segal method, which was 61%. Comparison of the degree of crystallinity of the initial cellulose sample with that of cellulose with the embedded nanoAg indicates a negligible increase in the degree of crystallinity of the cellulose sample with the embedded silver nanoparticles. Due to the significant difference in the size of cellulose and silver nanoparticles, for energy calculations there was used the following system: a spherical nanoAg particle and a flat cellulose particle. The dispersion interactions were determined based on the Hamaker's constant value, which for the suspension system containing cellulose particles and silver nanoparticles was $1.36 \cdot 10^{-20}$. Based on the values of the Hamaker constants and the zeta potential based on the DLVO theory, the interactions energy of the cellulose particles and the Ag nanoparticles was calculated. The results showed that the total energy of the interactions is close to that of the dispersion interactions (attractive forces predominate) and the electrostatic interactions are attractive and do not prevent aggregation.

References

BISWAS P. Kr., DEY S., 2015. *Effects and Applications of Silver Nanoparticles in Different Fields.* Int. J. Recent Sci. Res. 6(8), 5880-5883.

BURDUSEL A.C., GHERASIM O., GRUMEZESCU A.M., MOGOANTA L., FICAI A., ANDRONESCU E., 2018. *Biomedical Applications of Silver Nanoparticles: An Up-to-Date Overview.* Nanomat. 8, 681.

DĘBEK P., FELICZAK-GUZIK A., NOWAK I., 2017. *Nanostruktury – ogólne informacje. Zastosowanie nanoobiektów w medycynie i kosmetologii. Postepy.* Hig. Med. Dosw. 71, 1055-1062.

GU Y., LI D., 1999. *The van der Waals Interactions between a Spherical Particle and Cylinder.* J. Colloid Interface Sci. 217, 60-69.

GUPTA A., TURNER S.R. 2017. *Cellulose.* University of Manchester.

KOBAYASHI Y., MAEDA T., YASUDA Y., MORITA T., 2016. *Metal–metal bonding using silver/copper nanoparticles.* Appl. Nanosci. 6, 883–893.

LANGAUER-LEWOWICKA H., PAWLAS K., 2014. *Nanocząstki, nanotechnologii – potencjalne zagrożenia środowiskowe i zawodowe.* Eviron. Med. 17(2), 7-14.

LAVOINE N., DESLOGES I., DUFRESNE A., BRAS J., 2012. *Microfibrillated cellulose – Its barrier properties and applications in cellulosic materials: A review.* Carbohydrate Polymers 90, 735– 764.

PULIT J., BANACH M., KOWALSKI Z., 2011. *Właściwości nanocząsteczek miedzi, platyny, srebra, złota i palladu*. Chemia. Czasopismo Techniczne 2-Ch/2011, 198-209.

RUNOWSKI M., 2014. *Nanotechnologia – Nanomateriały, nanocząstki i wielofunkcyjne nanostruktury typu rdzeń/powłoka.* Chemik 68, 9, 766–775.

RZESZUTEK J., MATYSIAK M., CZAJKA M., SAWICKI K., RACHUBIK P., KRUSZEWSKI M., KAPKA-SKRZYPCZAK L., 2014. *Zastosowanie nanocząstek i nanomateriałów w medycynie.* HYGEIA Public Health 49(3), 449-457.

SEGAL L., CREELY J. J., MARTIN A. E., CONRAD C. M., 1959. *An empirical method for estimating the degree of crystallinity of native cellulose using the x-ray diffractometer.* Tex. Res. J. J29, 786–794.

SKIBA M., VOROBYOVA V., PASENKO O. 2022. *Surface modifcation of titanium dioxide with silver nanoparticles for application in photocatalysis.* Appl. Nanosci. 12, 1175–1182.

ZHANG X.F., LIU Z.G., SHEN W., GURUNATHAN S., 2016. *Silver Nanoparticles: Synthesis, Characterization, Properties, Applications, and Therapeutic Approaches.* Int. J. Mol. Sci. 17, 1534.

ZIENKIEWICZ-STRZAŁKA M., DERYŁO-MARCZEWSKA A., KOZAKEVYCH R.B., 2018. *Silica nanocomposites based on silver nanoparticles-functionalization and pH effect.* Appl. Nanosci. 8, 1649–1668.

ZIENKIEWICZ-STRZAŁKA M., PIKUS S., 2013. *Synthesis of photoactive AgCl/SBA-15 by conversion of silver nanoparticles into stable AgCl nanoparticles*. Appl. Surf. Sci. 265, 910.